International Journal of Engineering & Technology, 7 (4.8) (2018) 618-624

International Journal of Engineering & Technology

Website:www.sciencepubco.com/index.php/IJET

Research paper

Analysis of Heat-Insulating and Structural Building Members Behavior by the Finite Element Method

Oleksandra Cherednikova[1*], Yurii Avramenko[2], Olesia Rozdabara[3], Vitaliy Lapchuk[4]

[1]*Poltava National Technical Yuri Kondratyuk University, Ukraine*
[2]*Poltava National Technical Yuri Kondratyuk University, Ukraine*
[3]*Poltava National Technical Yuri Kondratyuk University, Ukraine*
[4]*National University of Water and Environmental Engineering, Ukraine*
**Corresponding author E-mail: al.chered108@gmail.Com*

Abstract

The paper deals with research of heat-insulating and structural elements in modern construction of Ukraine. It is established that the obtaining of theoretical models for the calculation of such type of structural elements is an economically important task that needs to be solved. The work of light polystyrene concrete slabs with profiled flooring and with different types of anchoring by finite element method (FEM) has been investigated. The method of plate models constructing for detailed study of the profiled flooring work, the material contact, their bundle, as well as the work of the reinforcement and its influence on the parameters of the stress-deformed state of polystyrene concrete and profiled flooring was proposed. Samples of light polystyrene concrete slabs with profiled flooring with different types of anchoring with the best stress-strain state characteristics were determined. The adequacy of the FEM models of plates was confirmed by comparing the results of the calculation with theoretical studies.

Keywords: *deformation property, finite element method (FEM), light concrete composite slabs, load, reinforcement, thermal insulation structure.*

1. Introduction

The most important issue that arises from the rise in prices for energy resources and the annual decline in natural resources is the use of heat-insulating, energy-efficient structures in the construction of both Ukraine [16] and any other country in the world. Taking into account this factor, we consider light concrete composite slabs with profiled flooring [6, 10] as structures that have not only high design qualities but also thermal insulation qualities. Ideally, the plates of the flooring and slabs should be light, but along with this must have high strength, low deformability and a small coefficient of thermal conductivity. Light concrete slabs in which light concrete will work together with profiled flooring can combine all of the above qualities. First you need to determine the type of connection used. The second problem arises from the fact that experimental design studies always require significant financial costs, so there is a need for analytical calculations that can describe the work of various types of light concrete slabs with profiled flooring under load.

The scientific research in the field of construction was devoted to application of various types of anchoring and reinforcement in composite structures. But mostly in these constructions heavy concrete was used but not light. Belyaev S.Yu., Darienko V.V., Skyba O.V. and other scholars has given enough attention to this issue [1, 2, 3]. Avramenko Yu.O., Semko O.V. and other were engaged in investigations of polystyrene concrete samples depending on the strength class of concrete, taking into account the stability of the profile in the steel-concrete samples [4, 5, 11].

The engineering methods that exist to date are designed only for heavy concrete structures, but do not allow to investigate the stress-strain state, both reinforcement and concrete, since they are intended only for testing strength and deformability. Analytical methods for calculating composite slabs [2, 9] only to some extent describe the work of the panels being considered. This is due to the fact that various assumptions or hypotheses about the nature of plates deformation are used to obtain finite equations.

Numerical methods based on the direct solution of the elasticity theory equations are devoid of most of these disadvantages. [12, 17]. Depending on the considered tasks these methods can be used both for the study of the SSS (stress-strain state) of plates, and for their simplified engineering calculations.

Based on the above facts, it was decided to conduct a study of light concrete slabs with different types of anchors and without anchors by the finite element method (FEM). Different approaches and methods of simulation of constructions, nodes by FEM are widely presented in the scientific works of world scholars [7, 8, 14, 15, 17].

The task of the presented work consists of the following stages: creating of three-dimensional geometric models of profiled flooring, polystyrene concrete and contact; defining of physical and mechanical models of materials and contact work; building a grid of finite elements; applying loads and boundary conditions; defining the type of calculation and analysis of the data. As the beginning of this work the PMA-2 plate was studied by FEM in detail and a step-by-step description of the simulation process is described in [9].

2. Main body

Construction of FEM models of light concrete slabs with profiled flooring was based on experimental models of these slabs. Six types of plates were experimentally investigated, the detailed description of which is given in previous works [6, 10]:

1) PM-1 sample is monolithic polystyrene concrete slab with profiled flooring without anchoring [10, 13];

2) PMA-1, PMA-4, PMA-5 samples are monolithic polystyrene concrete slabs with profiled flooring and vertical bolted anchoring with different number of bolted joints (4, 12, 8 pieces respectively);

3) PMA-2 sample is monolithic polystyrene concrete slab with profiled flooring with flexible anchors, located vertically and at an angle ±25° from the vertical [9];

4) PMA-3 sample is monolithic polystyrene concrete slab with profiled flooring with horizontal anchors in the form of transverse reinforcement that cross the walls of profiled flooring.

Linear and nonlinear static calculations were performed for all the models. In the linear static calculation, the nonlinear properties of materials and the geometric nonlinearity of the design were ignored. The calculation was made on the initial modules of elasticity. Nonlinear calculation involves applying the load in several steps, increasing it from zero to maximum value. At each step of the load, the values of the modulus of the elasticity were calculated, according to the deformation diagrams of the materials. This process end when the maximum load was reached or when the structure was transformed into a mechanism there appears plastic hinged point, lost local or general stability, etc. In all nonlinear calculations, the number of load steps was 20, but not all plates reached the maximum load value.

PM-1 plate. The results of the nonlinear calculation of PM-1 plates at the maximum load are shown in Figure 1. The maximum deflections in the middle of the span determined at the location of the leverarm deflection indicator, are presented in Table 1.

Figure 1 shows a diagram of the Mises stresses distribution and the nature of deformation of polystyrene concrete in the nonlinear calculation. In the distribution of stresses there are no peculiarities and it is similar to the distribution of stresses in linear calculation, and in general corresponds to the picture of stress distribution at bending.

The shape of the deformation of the profiled flooring in a nonlinear calculation differs from the linear due to the segregation of materials and separated work of profiled flooring and polystyrene concrete after segregation.

At the first stages of the $0{,}1F_{\max}$ load there is no segregation and the contact works like polystyrene concrete, with the $0{,}25\,F_{\max}$ elongation of loading on structure and more there is a segregation of materials. As the load increases, the contact zone decreases, starting from the reference and central zones and ending with the lateral surfaces of the profiled flooring in the middle of the slab span. Under $0{,}5\,F_{\max}$ load were a complete segregation of materials. Further deformation of the components of the plate occurred differently for different zones of the slab. So in the reference zones the separation of the profiled flooring from the concrete increased, while in the middle of the span, both materials deformed the same, although they were not combined, and only at maximum load their final segregation occurred, as evidenced by the schedule of deflections in Figure 2.

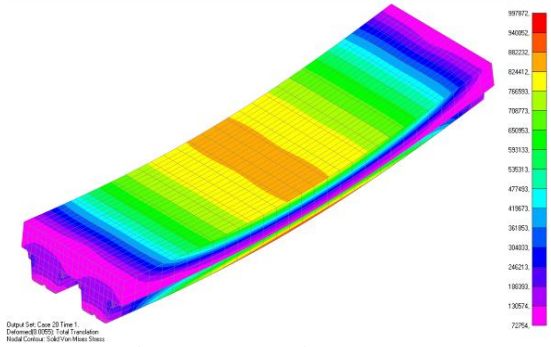

Fig. 1: - Diagram of the distribution of Mises stresses and the nature of deformation of polystyrene concrete in the nonlinear calculation of the PM-1 plate

In the analysis of the Mises stress distribution diagrams and the pattern of deformation of polystyrene concrete and profiled flooring during linear calculation of plates, it was discovered that the linear calculation does not allow to detect the effects of segregation or bending of profiled flooring radii. In this case, the components of the plate work as one by the initial modules of the elasticity of the materials. Such a reflection of the process increases the stiffness and durability of the structure, and as a result shows less deflections and stresses than the experimental maximum.

In order to compare the deflections with the experiment and the study of contact work in the models of FEM, pairs of adjacent nodes were selected which corresponded to the position of the leverarm deflection indicators and belonged to the polystyrene concrete and profiled flooring. Such nodes were located one above the other at a distance of contact. This allowed to precisely determine the moment of materials separate work beginning after segregation. Subsequently, for the generalization of the results, the comparison was performed not for one node, but for a pair of adjacent nodes.

Linear calculation for both adjacent nodes yields exactly the same results so the results of the calculation indicated the value of the deflections only for one of the nodes.

For the PM-1 plate, the nodes 3246 and 1262 were adjacent nodes. The first belonged to polystyrene concrete, and the second to profiled flooring. Table 1 shows the results of nonlinear and linear calculations of deflections, and in Figure 2, according to these data, a corresponding graph is constructed.

Table 1: Results of deflections for PM-1 plate by FEM

Load step	Load, N	Deflection, mm		
		Node 3246	Node 1262	Linear calculation
0	0	0	0	0
1	591	0,16	0,16	0,15
2	1182	0,31	0,31	0,30
3	1773	0,47	0,47	0,46
4	2364	0,63	0,63	0,61
5	2955	0,80	0,80	0,76
6	3546	0,98	0,98	0,91
7	4137	1,18	1,18	1,06
8	4728	1,41	1,41	1,22
9	5319	1,64	1,64	1,37
10	5911	1,88	1,88	1,52
11	6502	2,12	2,12	1,67
12	7093	2,37	2,37	1,82
13	7684	2,61	2,61	1,98
14	8275	2,87	2,87	2,13
15	8866	3,13	3,13	2,28
16	9457	3,44	3,44	2,43
17	10048	3,73	3,74	2,58
18	10639	4,02	4,03	2,74
19	11230	4,31	4,33	2,89
20	11821	5,43	4,59	3,04

From the analysis of the data presented in Table 1 and in Figure 2, we conclude that the account of nonlinearity significantly affects the calculation results. Deflections was increased by an average of 64% during nonlinear calculations. The diagram clearly demonstrates the nonlinear operation of the plate and at the maximum load, the separation of the profiled flooring and polystyrene concrete occurs.

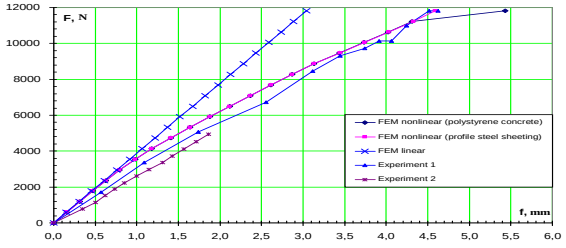

Fig. 2: The dependence of the deflections on the mid-pass load for the PM-1 plate according to the FEM calculations and experimental data

With regard to stresses, they are increased by 35% in polystyrene concrete, and by more than 250% in steel reaching the yield stress in comparison with the linear calculation.

PMA-1, PMA-4, PMA-5 plate. PMA-1 plate was calculated with two variants of finite element for modeling of profiled flooring as two- and three-dimensional to determine the most effective modeling technique for profiled flooring. In both cases, during a nonlinear calculation, it was not possible to reach the maximum experimental load value. In 2D FE modeling calculation ended at the value $0{,}75625F_{max}$ and in 3D FE modeling calculation ended at the value $0{,}829687F_{max}$. The reason for stopping the calculation was the loss of local stability of profiled flooring shelves. However, in the case of 3D FE, it was possible to visually capture the start of buckling (Figure 4), which doesn`t happen when using 2D FE. Calculations of plates with both FE variants showed (see Table 2) that the use of 2D or 3D FE does not significantly affect the results.

Based on the results obtained for the PMA-1 plate, it was decided to apply 3D FE to the modeling of profiled flooring in other plates.

Results of nonlinear calculation of PMA-1, PMA-5, PMA-4 plates at maximum load are shown in Figures 3-4. The maximum deflections determined in the middle of the span at the location of the leverarm deflection indicator are given in tables 2-3.

Figure 3 shows a diagram of Mises stresses distribution and the nature of polystyrene concrete deformation in the nonlinear calculation of PMA-1, PMA-5, PMA-4 plates. As you can see, the amount of vertical armature practically does not affect the stress-strain state of the plates, but has a small effect on the deflections. On all plates there is clearly a concentration of stresses on the edges that simulate the "boards". Moreover, under the very "board" the stress is much smaller than the stress across its edges. In support zones stresses reached critical values of 1 MPa at a load of about 6000 N, while in the middle of the span with a load of 12,000 N. A further increase in the load increased the size of the zones with the maximal stresses.

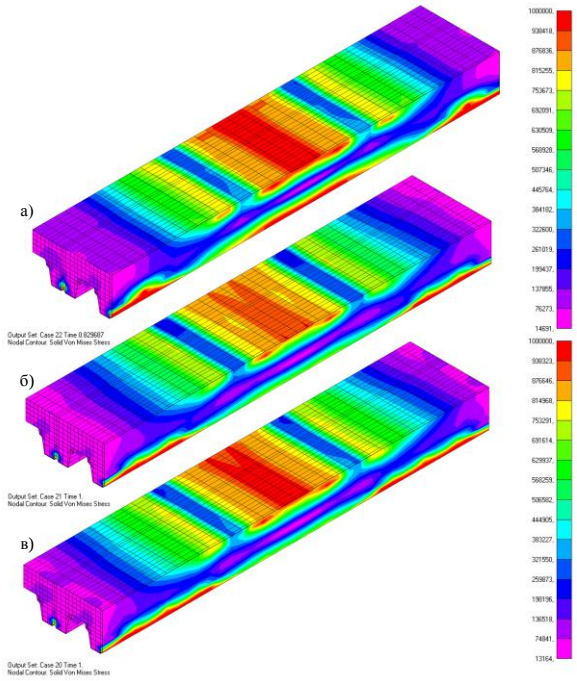

Fig. 3: Distribution of Mises stresses along the longitudinal cross-section of polystyrene concrete on reinforcement for plates PMA-1 (а), PMA-5 (б) і PMA-4 (в)

Figure 4 shows the distribution of Mises stresses and the nature of deformation of profiled flooring when non-linear calculation for PMA-1, PMA 5, PMA-4 plates. Just as for polystyrene concrete the amount of vertical reinforcement affects only the deformed state.

The work of the armature is shown in Figure 5. As the figure shows, the stress-strain state of armature was directly dependent on its quantity. In the PMA-1 plate, the stress reached a yield strength in two FEs on the armature branch; for PMA-5 plate in one FEs; for PMA-5 plate in no one FEs. The same applies to deformations, in plates with the least amount of reinforcement, the latter most curved and vice versa. From the analysis of Figure 5 we come to the conclusion that the reinforcement only works in the lower half of the plate, where there are large tangential stresses. Therefore, from a practical point of view, it is advisable to lay such fittings in lengths not more than 2/3 of the height of the profiled flooring.

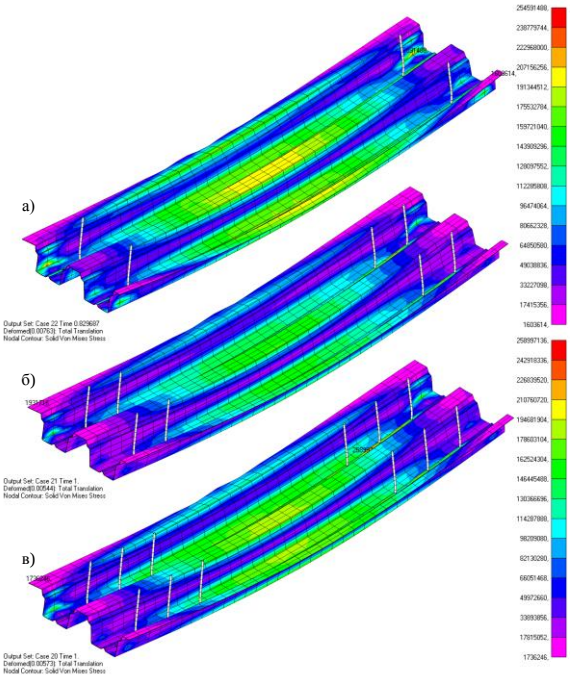

Fig. 4: Diagram of stress distribution Mises and the nature of deformation of profiled flooring during nonlinear calculation for plates PMA-1 (а), PMA-5 (б) і PMA-4 (в)

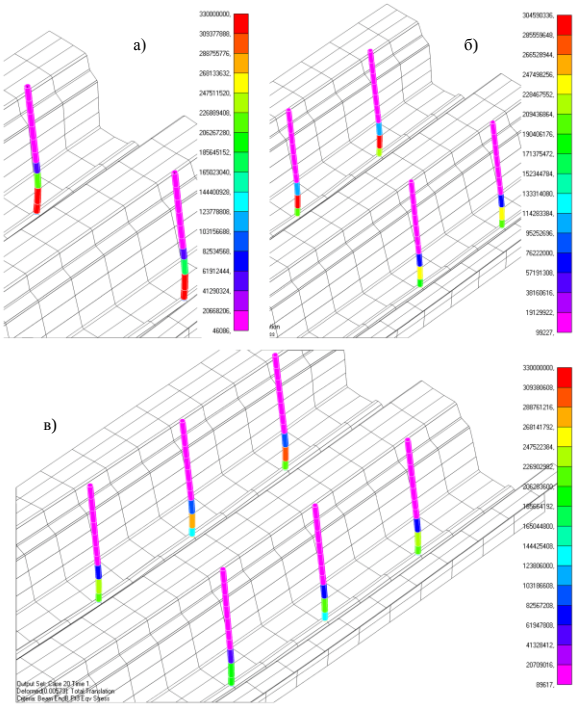

Fig. 5: Diagram of the distribution of stresses Mises and the nature of the deformation of the armature in the nonlinear calculation for plates PMA-1 (а), PMA-5 (б) і PMA-4 (в)

Table 2 shows the results of a comparative calculation of PMA-1 plate deflections when applying 2D and 3D CEs for profiled flooring. Gaps in load levels correspond to the stages when an intermediate calculation was required due to insufficient convergence. As you can see, the number of such stages in the case of 2D FE is much higher. Accordingly, the use of 3D FE is more attractive. The largest difference between the two calculations reached an average of 0.435 mm (8%) for nonlinear calculation and 0.02 mm for linear.

Table 2: Comparison of PMA-1 plate deflection results using 2D and 3D FE for profiled flooring simulation

Step load	Load, N	Deflection of PMA-1 slab (3D), mm			Deflection of PMA-1 slab (2D), mm		
		Node 19406	Node 3595	Linear calculation	Node 19406	Node 3595	Linear calculation
0	0	0	0	0	0	0	0
1	824	0,23	0,23	0,23	0,23	0,23	0,23
2	1648	0,46	0,46	0,46	0,46	0,46	0,46
3	2472	0,70	0,70	0,69	0,70	0,70	0,69
–	2884	–	–	–	0,81	0,81	0,80
5	3296	0,95	0,95	0,93	0,94	0,94	0,92
6	4120	1,23	1,23	1,16	1,22	1,22	1,15
7	4944	1,53	1,53	1,39	1,52	1,52	1,38
8	5768	1,85	1,85	1,62	1,84	1,84	1,61
9	6592	2,19	2,18	1,85	2,18	2,18	1,84
10	7416	2,54	2,51	2,08	2,53	2,51	2,07
11	8240	2,90	2,84	2,31	2,90	2,86	2,30
12	9064	3,28	3,19	2,55	3,34	3,25	2,53
13	9888	3,72	3,56	2,78	3,77	3,63	2,76
–	10712	4,15	3,93	3,01	4,41	3,75	2,99
14	11124	4,59	3,73	3,12	4,66	3,95	3,10
–	11330	–	–	–	5,33	4,20	3,16
–	11536	5,36	4,12	3,24	5,45	4,29	3,22
17	12360	5,84	4,48	3,47	5,96	4,69	3,45
–	12412	–	–	–	6,00	4,72	3,46
–	12437	–	–	–	6,02	4,73	3,47
–	12463	–	–	–	6,03	4,75	3,48
18	13184	6,38	4,85	3,70	–	–	–
–	13390	6,52	4,95	3,76	–	–	–
–	13596	6,66	5,04	3,82	–	–	–
–	13622	6,68	5,06	3,82	–	–	–
–	13648	6,70	5,07	3,83	–	–	–
–	13673	6,75	5,09	3,84	–	–	–
–	16480	–	–	4,63	–	–	4,60

The results of calculating PMA-5 and PMA-4 plates are summarized in Table 3.

Table 3: Comparison of calculation results of plates deflections for PMA-5 and PMA-4

Step load	Deflection of PMA-5, mm				Deflection of PMA-4, mm			
	Load, N	Node 19367	Node 19013	Linear calcula-tion	Load, N	Node 19367	Node 19013	Linear calcula-tion
0	0	0,00	0,00	0	0	0,00	0,00	0
1	624	0,18	0,18	0,18	674	0,19	0,19	0,19
2	1248	0,35	0,35	0,35	1348	0,38	0,38	0,38
3	1872	0,53	0,53	0,53	2022	0,57	0,57	0,57
4	2496	0,71	0,71	0,70	2696	0,77	0,77	0,76
5	3120	0,89	0,89	0,88	3370	0,97	0,97	0,95
6	3744	1,09	1,09	1,05	4044	1,18	1,18	1,14
7	4368	1,30	1,30	1,23	4718	1,41	1,41	1,33
8	4992	1,51	1,51	1,40	5392	1,63	1,63	1,52
9	5616	1,73	1,73	1,58	6066	1,87	1,86	1,70
10	6240	1,96	1,95	1,75	6740	2,10	2,10	1,89
11	6864	2,19	2,17	1,93	7414	2,34	2,33	2,08
12	7488	2,43	2,40	2,10	8088	2,59	2,56	2,27
13	8112	2,68	2,62	2,28	8762	2,85	2,80	2,46
14	8736	2,94	2,85	2,45	9436	3,12	3,04	2,65
15	9360	3,21	3,08	2,63	10110	3,40	3,29	2,84
16	9984	3,49	3,32	2,81	10784	3,69	3,53	3,03
17	10608	3,81	3,57	2,98	11458	4,03	3,80	3,22
18	11232	4,12	3,82	3,16	12132	4,35	4,07	3,41
19	11856	4,51	3,94	3,33	12806	4,68	4,32	3,60
–	12168	4,81	3,83	3,42	–	–	–	–
20	12480	4,98	3,95	3,51	13480	5,22	4,26	3,79

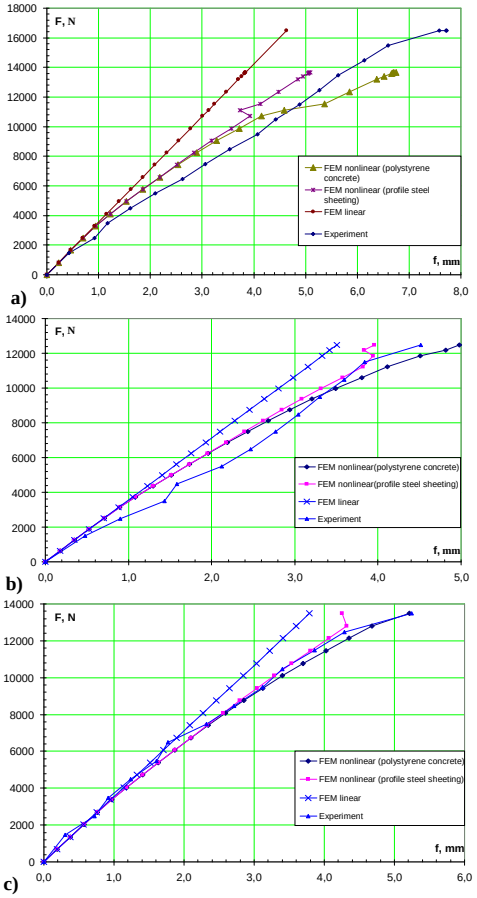

Fig. 6: Comparison of plate deflections PMA-1(a), PMA-5(b), PMA-4(c)

Figure 6 presents the results of a comparative analysis of calculations PMA-1, PMA-5 and PMA-4 plate deflections presented in Tables 2 and 3 using 3D FE which simulates the profiled flooring. As you can see, the calculations on the linear model completely coincide with each other, once again confirming the fact that the number of armature does not affect the work of the plate at a linear calculation. In a nonlinear calculation, the situation is somewhat different, but the overall conclusion remains the same.

Plate PMA-2. When calculating the PMA-2 plate, as well as for the PMA-1 plate, it was not possible to achieve maximum experimental load. Calculation ended on value $0{,}8F_{max}$. Results of nonlinear calculation of PMA-2 plates at maximum load are shown in the figures 7-8. More information on modeling and analyzing the work of the PMA-2 plate is provided in [9].

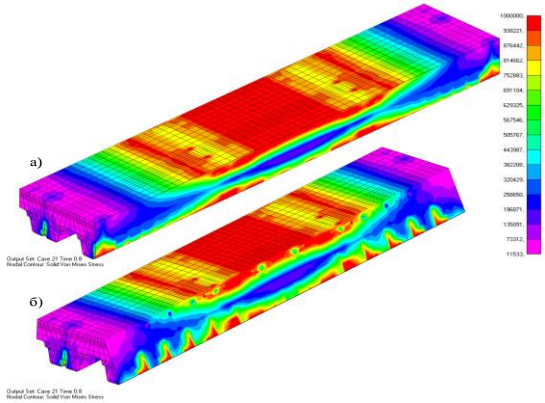

Fig. 7: Influence of vertical and inclined armature on the stress condition of the PMA-2 plate: а) longitudinal vertical section on reinforcement;б) longitudinal inclined section on reinforcement

Figure 7 shows a diagram of the distribution of Mises stresses and the nature of polystyrene concrete deformation in a nonlinear calculation in a PMA 2 plate. On the upper surface of polystyrene concrete near the armature location there are small concentrations of stress. There are also concentrations of stresses from the action of loads through absolutely rigid finite elements, as well as in the PMA-1, PMA-5, PMA-4 plates.

Figure 8 is a graph of deformation of the PMA-2 plate. The main difference from the previous results is that in the process of segregation occurs almost without jumps of deformation. This is due to the increased stiffness of the plate. The separation of the polystyrene concrete from profiled flooring begins at a load of 12,000 N and the distance between the adjacent knots begins to smoothly increases with increasing load.

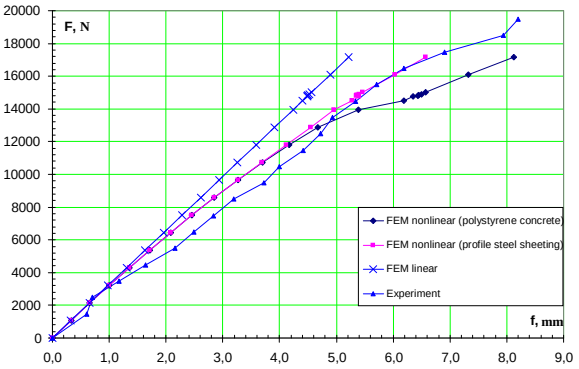

Fig. 8: deflections dependence on the load in the middle of the span for plate PMA-2

Plate PMA-3. Results of nonlinear calculation of PMA-3 plates at maximum load are shown in Figures 9-10. The maximum deflections determined in the middle of the span at the location of the leverarm deflection indicator are given in Table 4. As the results of the calculation show the PMA-3 plate has the highest rigidity among all the considered plates. The pattern of stress distribution on the upper edge of polystyrene concrete and on the stove in general is similar to the pattern of stress distribution with classical calculation methods. the zone of greatest stress corresponds to the location of the maximum moment; stress concentration under absolutely rigid finite elements are small and practically absent. The same applies to the profiled flooring work (Figure 10). On the lateral surfaces of polystyrene concrete the horizontal section of the increased stresses, which corresponds to the position of the horizontal armature, is clearly distinguished.

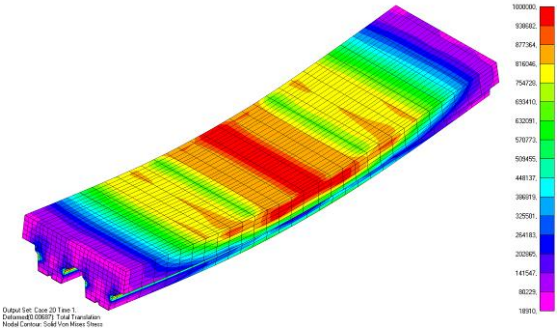

Fig. 9: Diagram of the distribution of Mises stresses and the nature of deformation of polystyrene concrete in the nonlinear calculation of PMA-3 plate

The stresses in reinforcement and profiled flooring did not reach the limit values (Figure 11), which indicates their elastic work up to the maximum load. The stresses between individual armature were evenly distributed with some increasing in the support zones. Distribution of stresses on the armature itself was uneven. The greatest stresses arose on the edge of contact with the profiled flooring and sharply decreased in the distance from the profiled flooring. The maximum dimensions of such zones were 1/6 of the armature length. In the middle part the armature did not work.

Based on the results of the conducted studies it can be considered that the anchoring method used in the PMA-3 plate is most effective since the plate has the highest rigidity and does not has significant stress concentrations caused by the work of the reinforcement.

During the experiment and in calculations, the values of the deflections in the middle of plates and profiled flooring were obtained. Since in nonlinear calculations at the maximum load in all cases, except for the PMA-3 plate there was a segregation of profiled flooring from polystyrene concrete, then for comparison the averaged data of deflections on adjacent pairs of nodes was conducted. The approximation of the data was performed for correct results comparison. Load for different plates was reduced to the least destructive load (PM-1 plate, 11821 N). The data of the comparative analysis are presented in Table 5.

Table 4: Results of deflections calculation for PMA-3 plate

Step load	Load, N	Deflection of PMA-3, mm		
		Node 13461	Node 37236	Linear calculation
0	0	0,00	0,00	0
1	924	0,30	0,30	0,30
2	1848	0,59	0,59	0,59
3	2772	0,89	0,89	0,89
4	3696	1,20	1,20	1,18
5	4620	1,50	1,50	1,48
6	5544	1,81	1,81	1,77
7	6468	2,11	2,11	2,07
8	7392	2,42	2,42	2,36
9	8316	2,73	2,73	2,66
10	9240	3,05	3,05	2,96
11	10164	3,37	3,38	3,25
12	11088	3,70	3,71	3,55
13	12012	4,04	4,04	3,84
14	12936	4,38	4,39	4,14
15	13860	4,75	4,75	4,43
16	14784	5,12	5,12	4,73
17	15708	5,50	5,51	5,03
18	16632	5,91	5,91	5,32
19	17556	6,33	6,34	5,62
20	18480	6,78	6,78	5,91

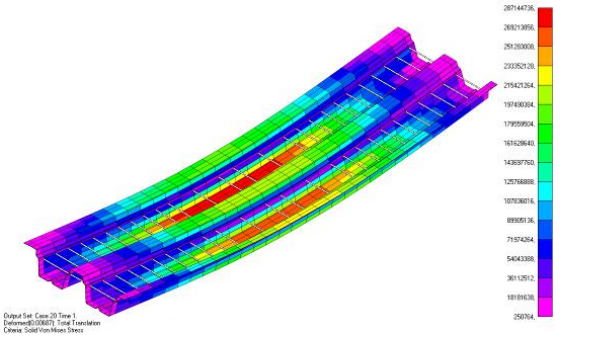

Fig. 10: Diagram of the distribution of Mises stresses and the nature of the deformation of the profiled flooring in the nonlinear calculation of the PMA-3

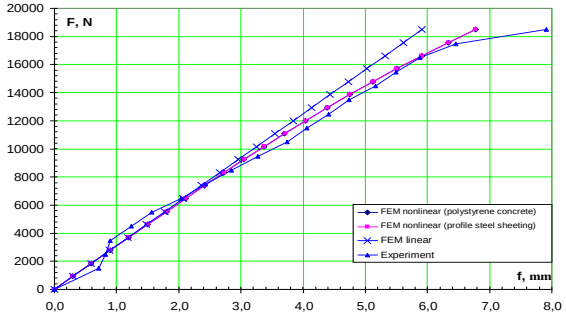

Fig. 11: The deflections dependence on the load in the middle of the span for the PMA-3 plate

3. Conclusions

The paper presented results of building and nonlinear calculating of light concrete plates by FEM. As can be seen from the results of the presented material, the nonlinear calculation of structure by FEM allows for a complete detailed analysis of the structure, to identify its weaknesses without resorting to experiments that take up a large amount of time and material resources. The performed calculations allow us to investigate the work of the profiled flooring, the contact of materials, their segregation, and also the work of the armature and its influence on the parameters of the stress-strain state of polystyrene concrete and profiled flooring. Accordingly, the following studies have developed practical recommendations for the simulation by FEM and calculation of light concrete plate with profiled flooring, which are partly presented in [9].

With regard to the choice of the anchoring method and the number of fittings, the most effective method is the anchoring used in the PMA-3 plate. The method of anchoring the plate PMA-2 cannot be considered successful, in terms of deformations and the number of used fittings. Therefore, the method of anchoring the plate used in PMA-2 can be recommended for use in cases where it is necessary to significantly increase the bearing capacity due to a slight decrease in the deformation properties of the plate. To improve the deformation properties of plates with sufficient bearing capacity, an anchoring similar to PMA-1, PMA-5, PMA-4 boards can be used, but only under such conditions and in no other way.

Table 5: Comparison of calculation results for plates PM-1, PMA 1 ... PMA-5 with experimental data under load 11821 N

Type of plate	Experimental	Nonlinear calculation					Difference, %	Linear calculation	Difference, %
	Deflection, mm	Node #	Deflection, mm	Node #	Deflection, mm	Average, mm		Deflection, mm	
PM-1	*4,63*	3246	5,43	1262	4,59	*5,01*	*8,2*	*3,04*	*34*
PMA-1	*5,01*	19406	5,53	3595	4,25	*4,89*	*2,4*	*3,32*	*34*
PMA-5	*4,07*	19367	4,49	19013	3,94	*4,21*	*3,4*	*3,32*	*18*
PMA-4	*4,01*	19367	4,20	19013	3,95	*4,07*	*1,5*	*3,32*	*17*
PMA-2	*4,52*	1261	4,17	2149	4,12	*4,14*	*8,4*	*3,59*	*21*
PMA-3	*4,18*	13461	3,97	37236	3,97	*3,97*	*5,0*	*3,78*	*10*

Acknowledgement

The research was carried out in Poltava National Technical Yuri Kondratyuk University, and its key findings were implemented as part of state-financed applied scientific research works: “Estimation of reliability and risks of load-bearing structures and building envelopes" (state registration number 0111U000839), “Regulation of reliability and risks of building constructions” (state registration number (0113U000382), “Constructive and thermal reliability of bearing and envelope complex structures” (state registration number 0115U002417), “Resource-efficient technologies of renovation and reconstruction of residential, civil and industrial buildings and protective structures of civil defense” (state registration number 0116U002567).

References

[1] Belyaeva S. Yu. Eksperimentalnyie issledovaniya zhelezobetonnyih plit, armirovannyih stalnyim profilirovannyim nastilom. Zb. nauk. prats Donbas. tekhnichn. un-tu. Alchevsk. Vyp. 20, (2005), s. 344–348. http://nvd.luguniv.edu.ua/archiv/NN2/07busspn.pdf

[2] Koval M. P., Kondriukova I. O. Doslidzhennia roboty monolitnykh zalizobetonnykh plyt zi stalevym profilovanym nastylom N80A ta boltovymy opornymy ankeramy pry dii statychnoho y vysokorivnevoho malotsyklovoho navantazhennia. Zbirnyk naukovykh prats. Seriia: haluzeve mashynobuduvannia, budivnytstvo. Poltava. Vyp. 1(43), (2015), s. 170–177. http://journals.pntu.edu.ua/index.php/znp/article/view/121.

[3] Semko O. V., Krupchenko O. A., Dariienko V. V., Hlinkin M. I. Doslidzhennia napruzheno-deformovanoho stanu zalizobetonnykh rebrystykh plyt pokryttiv v rozrakhunkovomu kompleksi NASTRAN. Problemy rozvytku dorozhno-transportnoho i budivelnoho kompleksiv : zb. statei i tez Mizhnar. nauk.-prak. konf., 3 – 5 zhovtnia 2013 r. Kirovohrad. (2013), s. 358 – 363.

[4] Leshchenko M. V., Semko V. O. Thermal characteristics of the external walling made of cold-formed steel studs and polystyrene concrete. *Magazine of Civil Engineering*. № 8, (2015), pp. 44–55. https://doi.org/10.5862/MCE.60.6

[5] Semko O. V., Lazariev D. M., Avramenko Yu. O. Lehkyi beton dlia zapovnennia porozhnyn stalevykh tonkostinnykh konstruktsii. Zbirnyk naukovykh prats. K.: DP NDIBK. # 74, (2011), s. 659–666.

[6] Voskobiinyk O.P., Cherednikova O.V. Experimental study of the effect of anchorage on bearing capacity and deformation property of the light concrete composite slabs. *Stroitel'stvo, materialovedenie, mashinostroenie: collection of scientific papers.* Dnepr : PSACEA. Issue.. 100, (2017), c. 56–63. http://smm.pgasa.dp.ua/article/viewFile/113699/108264

[7] Akpoyomare A. I., Okereke M .I., Bingley M. S. Virtual testing of composites: Imposing periodic boundary conditions on general finite element meshes. *Composite Structures*. № 160, (2017), pp. 983–994. https://doi.org/10.1016/j.compstruct.2016.10.114.

[8] Carrazedo R., Coda H. B. Triangular based prismatic finite element for the analysis of orthotropic laminated beams, plates and shells. *Composite Structures*. № 168, (2017), pp. 234–246. https://doi.org/10.1016/j.compstruct.2017.02.027.

[9] Voskobiinyk O.P., Cherednikova O.V. Light concrete composite slab with flexible reinforcement stress-strain state modeling by finite element method. *Collection of scientific papers. Series: Haluzeve mashynobuduvannia, budivnytstvo.* Poltava. Issue 2 (49), (2017), c. 285–294. http://reposit.pntu.edu.ua/handle/PoltNTU/2845

[10] Cherednikov V., Voskobiinyk O., Cherednikova O. Evaluation of the warping model for analysis of polystyrene concrete slabs with profiled steel sheeting. *Periodica Polytechnica Civil Engineering*. №61(3), (2017), pp. 483–490. https://doi.org/10.3311/PPci.8717

[11] Semko O., Dariienko V., Sirobaba V. Deformability of short steel reinforced concrete structures on light concrete. *International Journal of Engineering & Technology*. Baku. Vol 7, No 3.2, (2018) pp. 370–375. https://www.sciencepubco.com/index.php/ijet/article/view/14555/5905

[12] Goncalves B.R., Karttunen A., Romanoff J., Reddy J.N. Buckling and free vibration of shear-flexible sandwich beams using a couple-stress-based finite element. *Composite Structures*. № 165, (2017), pp. 233–241. https://doi.org/10.1016/j.compstruct.2017.01.033.

[13] Voskobiinyk O.P., Cherednikova O.V. A determination of the parameters of stress-strained state of light concrete combined slabs for non-classical shear model. Зб. наук. праць Укр. держ. ун-ту залізнич. трансп. Харків: УкрДУЗТ,. Вип. 170, (2017), pp. 132–140. http://csw.kart.edu.ua/article/viewFile/111317/106315

[14] Han J.-W., Kim J.-S., Cho M. Improved finite element viscoelastic analysis of laminated structures via the enhanced first-order shear deformation theory. *Composite Structures*. № 180, (2017), pp. 360–377. https://doi.org/10.1016/j.compstruct.2017.07.099.

[15] Teng X. Zhang Y.X. Nonlinear finite element analyses of FRP-strengthened reinforced concrete slabs using a new layered composite plate element. *Composite Structures*. № 114, (2014), pp. 20–29. https://doi.org/10.1016/j.compstruct.2014.03.040

[16] Semko V., Leshchenko M., Cherednikova O. Standardization of required level probability of no-failure operation of the building envelopes by the criterion of total thermal resistance. *International Journal of Engineering & Technology*. Vol. 7 (3.2), (2018), pp 382-387.https://www.sciencepubco.com/index.php/ijet/article/view/14557

[17] Wan D., Hu D., Natarajan S., Stéphane P.A. Bordas., Long T. A linear smoothed quadratic finite element for the analysis of laminated composite Reissner–Mindlin plates. *Composite Structures.* № 180, (2017), pp. 395–411. https://doi.org/10.1016/j.compstruct.2017.07.092.

[18] Storozhenko L.I., Hasii H.M. The new composite designs for mine tunnel support. Naukovyi Visnyk Natsionalnoho Hirnychoho Universytetu. no. 4, (2015), pp. 28–34.
[19] Storozhenko L.I., Gasii G.M. Experimental research of strain-stress state of ferrocement slabs of composite reinforced concrete structure elements. Metallurgical and Mining Industry. Vol. 6, no. 6, (2014), pp. 40–42.
[20] Gasii G., Hasii O., Zabolotskyi O. Estimate of technical and economic benefits of a new space composite structure. MATEC Web of Conferences. Vol. 116, (2017), article number 02014. https://doi.org/10.1051/matecconf/201711602014
[21] Semko P. Comparison of experimental studies and numerical modeling results of concrete filled tubular elements with demountable joints / P. Semko / Serija: haluzeve mašynobuduvannja, budivnyctvo. – Vyp. 1(50).– Poltava, 2018. – S.88–97. http://reposit.pntu.edu.ua/handle/PoltNTU/3872